Proceedings of the XXI International Conference on Atomic Physics

PUSHING THE FRONTIERS OF ATOMIC PHYSICS

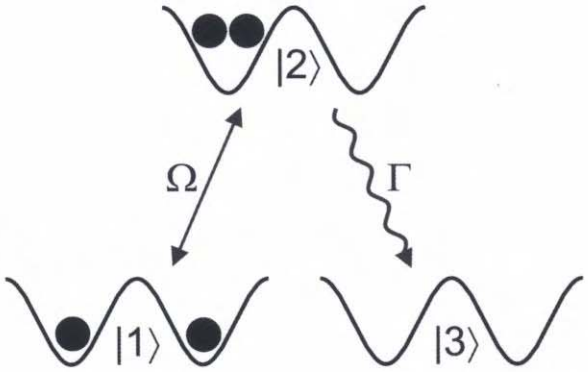

Robin Côté, Phillip L Gould,
Michael Rozman & Winthrop W Smith

editors

World Scientific

ATOMIC ENSEMBLE QUANTUM MEMORIES

S.-Y. LAN*, R. ZHAO*, S. D. JENKINS†, O. A. COLLINS*, Y. O. DUDIN*,
A. G. RADNAEV*, C. J. CAMPBELL*, D. N. MATSUKEVICH‡,
T. A. B. KENNEDY* and A. KUZMICH*

*School of Physics, Georgia Institute of Technology, Atlanta, Georgia 30332-0430
†CNR-INFM, Dipartimento di Fisica e Matematica,
Università degli Studi dell'Insubria, Via Valleggio 11 22100 Como, Italy
‡Department of Physics, University of Maryland, College Park, Maryland 20742

A key ingredient for a practical quantum repeater is a long memory coherence time. We describe a quantum memory using the magnetically-insensitive clock transition in atomic rubidium confined in a 1D optical lattice. We observe quantum lifetimes exceeding 6 milliseconds. We also demonstrate a dozen independent quantum memory elements within a single cold sample, and describe matter-light entanglement generation involving arbitrary pairs of these elements.

Keywords: Quantum memory; quantum repeater; matter-light entanglement.

1. Introduction

Quantum mechanics provides a mechanism for absolutely secure communication between remote parties, see for example Ref. 1. For distances greater than about a 100 kilometers direct quantum communication via optical fiber is difficult, due to fiber losses. To overcome this difficulty, intermediate storage of the quantum information along the transmission channel using a quantum repeater protocol has been suggested.[2] The optically thick atomic ensemble has emerged as an attractive medium for quantum storage, matter-light qubit entanglement generation and distribution.[3] Efficient quantum state transfer between ensemble-based qubits and single photons can be achieved in free space by utilizing a very weak interaction at a single photon/single atom level. The realization of coherent quantum state transfer from a matter qubit to a photon qubit was achieved using cold rubidium at Georgia Tech in 2004,[4] followed by the first light-matter qubit conversion and entanglement of remote atomic qubits in 2005.[5] A scheme to achieve long-distance quantum communication at the absorption minimum of

optical fibers, employing atomic cascade transitions, has been proposed and its critical elements experimentally verified.[6] In order to boost communication rates under conditions of limited quantum memory time, a modified quantum repeater based on dynamic allocation of quantum resources, multiplexed quantum repeater, has been proposed.[7]

Here we would like to report our recent progress on long-lived storage and retrieval of single quantum excitations, including a two order of magnitude increase in the quantum memory lifetime,[8] and the realization of multiple memory elements within a single cold atomic sample.

2. Long-lived quantum memory

Protocols for quantum communication are typically based on remote parties sharing and storing an entangled quantum state. The generation of such remote entanglement must necessarily be done locally and distributed by light transmission over optical fiber links or through free space.[16] For the distribution of entanglement over a length L the characteristic timescale for storage is the light travel time L/c, where c is the speed of light in the medium. For $L = 1000$ km, $L/c \approx 5$ ms for an optical fiber.

In recent advances involving atomic ensembles,[4–6,8–15] the quantum memory lifetime, was limited by residual magnetic fields, with the longest measured time of 32 μs.[8] To circumvent this limit one can use the ground-state hyperfine coherence of the $m = 0$ Zeeman levels as the basis of quantum storage. This so-called clock transition is only second-order sensitive to external magnetic fields, leading to a memory coherence time limit

$$\tau = [4\pi \cdot 575[\mathrm{Hz/G^2}]B_0 B' l]^{-1}.$$

Under our experimental conditions, with bias magnetic field $B_0 \sim 0.5$ G, gradient $B' \ll 30$ mG/cm, and sample length $l \sim 1$ mm, we find $\tau \gg 100$ ms.

Ballistic expansion of the freely falling gas provides a memory time limitation which can be estimated from the time $\tau = \Lambda/(2\pi v)$ it takes an atomic spin grating to dephase by atomic motion. For representative MOT parameters, grating wavelength $\Lambda = 50$ μm, atomic velocity $v = \sqrt{k_B T/M} \simeq 8$ cm/s for $T = 70$ μK, we find $\tau \sim 100$ μs. These estimates indicate that in order to demonstrate quantum memory lifetimes of many milliseconds we must suppress atomic motion and use a magnetically-insensitive atomic coherence as the basis of the quantum memory.

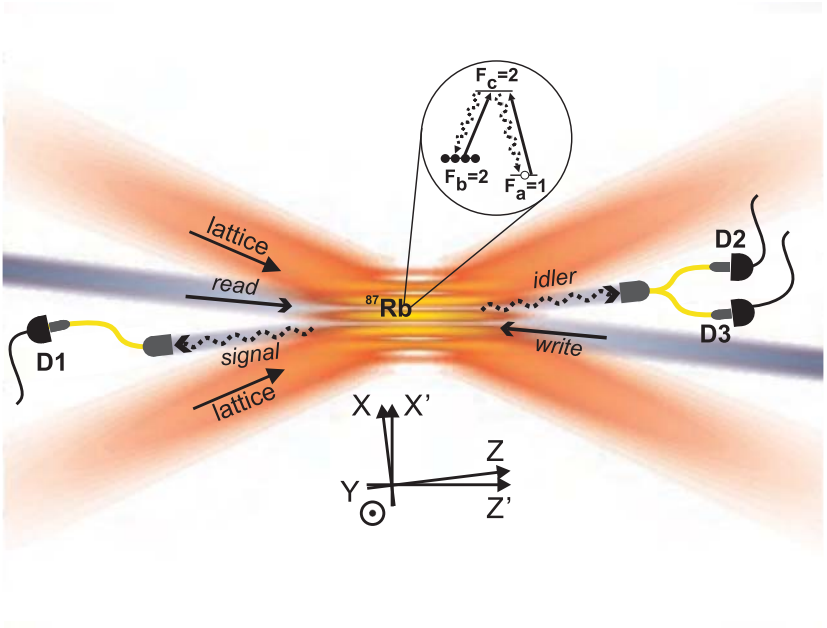

Fig. 1. Essential elements of the experimental set-up. Between 10^5 and 10^6 sub-Doppler cooled ^{87}Rb atoms are loaded into an optical lattice, and detection of the signal field generated by Raman scattering of the *write* laser pulse heralds the presence of a *write* spin wave excitation. A *read*/control field converts the surviving atomic excitation into an idler field after a storage period T_s. The inset shows the atomic level scheme of ^{87}Rb with levels a and b the hyperfine components of the ground $5S_{1/2}$ level, and level c a hyperfine component of the excited $5P_{1/2}$ level. The *write* laser excites the $b \leftrightarrow c$ transition, with Raman emission of the signal field on $c \rightarrow a$. The *read* laser excites the $a \leftrightarrow c$ transition, with Raman emission of the idler field on $c \rightarrow b$.

2.1. *Description of the system*

In order to suppress atomic motion, we load an atomic cloud of ^{87}Rb into a one-dimensional optical lattice, as shown in Fig. 1. The ground hyperfine levels a and b of ^{87}Rb have angular momenta $F_a = 1$ and $F_b = 2$, and the upper and lower clock states are written as $|+\rangle \equiv |b, m = 0\rangle$ and $|-\rangle \equiv |a, m = 0\rangle$, respectively. If the atoms are prepared in the upper clock state by optical pumping, the $|+\rangle$ and $|-\rangle$ states can be coupled by Raman scattering of a weak linearly polarized *write* laser field into an orthogonally polarized signal field detected in the near-forward direction. Ideally, after a controllable storage period, the *read* pulse converts atomic spin excitations into an idler field propagating along the quantization axis z, and linearly polarized in the x-direction. Under these conditions the medium

exhibits electromagnetically induced transparency with susceptibility for x-polarized idler field controlled by the read laser intensity

$$\chi_x(\Delta) = -\frac{1}{\omega_{cb}} \frac{n|\kappa|^2\Delta}{\Delta(\Delta + i\Gamma_c/2) - \frac{1}{2}|\Omega_r|^2},$$

where ω_{cb} is the transition frequency between levels c and b, Δ and Γ_c are the read laser detuning and spontaneous decay rate, Ω_r is the read laser Rabi frequency and $\sqrt{n}|\kappa|$ is the collective Rabi frequency, where n is the atomic density. The corresponding group velocity of the idler field is

$$v_g = c\frac{|\Omega_c|^2}{|\Omega_c|^2 + n|\kappa|^2}.$$

In order to maximize the retrieval efficiency, the signal and idler spatial mode functions should be matched and the condition $\mathbf{k_i} = \mathbf{k_w} - \mathbf{k_s} + \mathbf{k_r}$ satisfied, where $\mathbf{k_w}$, $\mathbf{k_s}$, $\mathbf{k_i}$ and $\mathbf{k_r}$ are wavevectors for the *write*, signal, idler and *read* fields, respectively.

The detection of the signal photon after a write pulse implies a momentum change $\hbar(\mathbf{k_w} - \mathbf{k_s})$ of the atoms (along the x′-axis). The excitation amplitude for an atom at position $\mathbf{r}$ is proportional to $e^{-i(\mathbf{k_w}-\mathbf{k_s})\cdot\mathbf{r}}$. Since the period of the lattice, 25 μm, is shorter than the spin grating wavelength $\Lambda \simeq \lambda/\theta \approx 50$ μm, determined by the angle $\theta \approx 0.9^\circ$ between the write and signal fields of wavelength $\lambda = 795$ nm, optical confinement helps to preserve the spin wave coherence by suppressing atomic motion along the $\mathbf{k_w} - \mathbf{k_s}$ direction.

2.2. *Retrieval of single quantum excitations*

We characterize how well the retrieved idler field compares to a single photon state by measuring the α-parameter of Grangier et al.,[18] which is defined by

$$\alpha = \frac{p_1 p_{123}}{p_{12} p_{13}}.$$

Here p_1, p_2, p_3 are the photoelectric detection probabilities on the three detectors, D1-3, respectively, Fig. 1. A field in a single-photon state incident on a beamsplitter is either transmitted or reflected, and the joint photoelectric detection probability vanishes, Fig. 2. The measured idler field is gated by detection of the signal field by D1.

In Table 1 we give the measured values of α, demonstrating quantum memory for storage times up to 6 ms. The value $\alpha = 0$ corresponds to an ideal, heralded single-photon state, whereas for classical fields $\alpha \geq 1$.

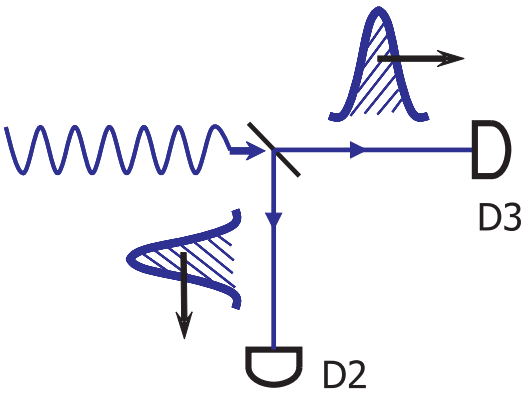

Fig. 2. A single photon incident on a beamsplitter takes one of two paths leading to anti-correlated photoelectron counting events at D2 and D3. This forms the basis of the α-parameter measurement scheme.[18]

Table 1. Measured values of α and intrinsic efficiency η_{int}.

storage time, ms	α	η_{int}
0.0012	0.02 ± 0.01	0.25
1	0.12 ± 0.04	0.11
4	0.17 ± 0.07	0.05
6	0.10 ± 0.10	0.045

Table 2. Measured values of $g_D^{(2)}$ and intrinsic source efficiency ϵ_{int}.

protocol duration, ms	$g_D^{(2)}$	ϵ_{int}
4	0.06 ± 0.04	0.08
5	0 ± 0.06	0.06

An important, immediate application of this long quantum memory is the realization of a deterministic single photon source based on quantum measurement and feedback, as proposed in Ref. 8. As the protocol's success is based on long memory times, we are now able to significantly improve the quality of the single-photon source. It is demonstrated by measuring sub-Poissonian photoelectron statistics of the second-order coherence function $0 \leq g_D^{(2)} < 1$, which is defined by

$$g_D^{(2)} = p_{23}/(p_2 p_3).$$

The source efficiency, defined as the probability ϵ to detect a photoelectric event per trial, is the second important figure of merit, ideally, $g_D^{(2)} = 0$

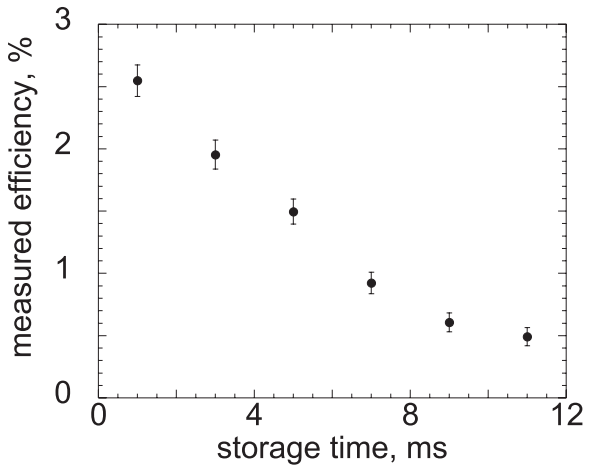

Fig. 3. Retrieval efficiency as a function of storage time for optically pumped atoms in an optical lattice with depth $U_0 = 40$ μK.

and $\epsilon = 1$. The measured passive losses from the atomic sample to the detector in the idler channel produce an efficiency factor of $0.25 \pm 10\%$. The measured values of $g_D^{(2)}$ and ϵ normalized by passive losses are given in Table 2.2.

In Fig. 3 we show the behavior of the measured retrieval efficiency — not normalized by passive losses — on the millisecond time-scale. The decay time is consistent with atomic motion in the lattice potential accompanied by differential light shifts of the clock states.[17]

3. Multiplexed quantum memory

The presence of multiple memory elements per node in a quantum repeater allows dynamic reallocation of resources improving the rate of quantum communication for short memory times.[7] Here we describe such a multiplexed quantum node. Individual addressing of memory elements within a single cold sample is achieved by means of 1D scanning with acousto-optical deflectors (AODs). This allows us to demonstrate matter-light entanglement using an arbitrary pair of memory elements in the array.

3.1. *Quantum memory array*

Our experimental setup is illustrated in Fig. 4. Two AODs are used to scan *write* and *read* beams, respectively. Each mode from the *write* AOD

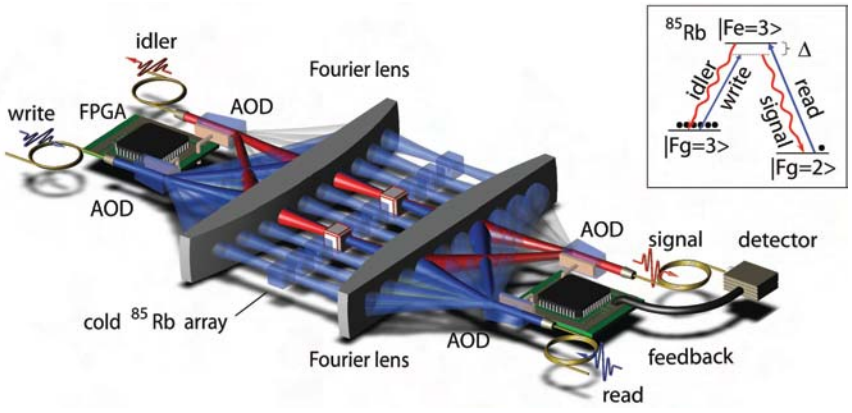

Fig. 4. Schematic illustration of the experimental setup for the multiplexed memory array. The inset shows the relevant ^{85}Rb energy levels.

is matched to the *read* AOD. Another two AODs are employed for the collection of the signal and idler fields. The phase matching condition $\mathbf{k}_w^{(j)} + \mathbf{k}_r^{(j)} = \mathbf{k}_s^{(j)} + \mathbf{k}_i^{(j)}$ is satisfied at each memory element address $j = 1 - 12$.

A field-programmable gate array (FPGA) controls addressing of the memory elements via a digital-to-analog converter. Sequential pulses generated by the control logic with different voltage levels are fed into a voltage-controlled oscillator (VCO) which converts them into rf pulses with different frequencies. After amplification these are directed into the write AOD, which produces *write* pulses into a set of spatial modes. These pulses enable individual addressing of a localized sub-region of the atomic cloud that forms a memory element.

Using a MOT, ^{85}Rb atoms are prepared in the $|5S_{1/2}, F = 3\rangle$ ground level. The protocol begins when the atoms are released from the trap. By electronic control the driving frequency of the *write* AOD is changed and within 1 μs the deflector points to the desired memory element. A 300 ns optical pulse, red detuned from the $|5S_{1/2}, F = 3\rangle \rightarrow |5P_{1/2}, F = 3\rangle$ transition by 10 MHz (we use an additional acousto-optical modulator to compensate the frequency shift of the write AOD), is then sent to the memory element. Synchronously the signal AOD directs the scattered signal field from the memory element to the single photon detector. In this way, a 12 pulse train scans the atomic array in temporal order with a time interval of 1.3 μs. The detection of the signal field in a specific gate interval of 250 ns indicates the origin of the signal field.

3.2. *Matter-light entanglement with a quantum memory array*

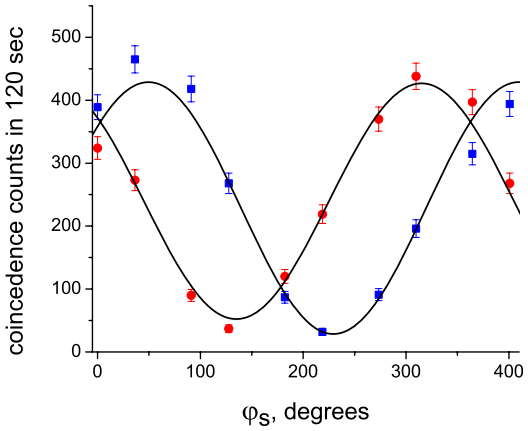

Fig. 5. Measured photoelectric coincidences for elements j=5 and 8 as a function of ϕ_s for $\phi_i = 0$, squares and $\phi_i = \pi/4$, circles. The solid curves are sinusoidal fits.

The AODs can be used as dynamic beam splitters, allowing to realize matter qubits based on pairs of elements of the memory array.

The write AOD aligned in +1 Bragg diffraction order is provided with two different rf frequencies, f_j and f_k ($f_j > f_k$), to generate two spatially distinct pulses. These two *write* pulses, red detuned from the $|5S_{1/2}, F = 3\rangle \rightarrow |5P_{1/2}, F = 3\rangle$ transition by -10 MHz and -10+(f_j-f_k) MHz, respectively, illuminate two different elements simultaneously. The signal fields are collected by the signal AOD, which is aligned and modulated, at frequencies f_j and f_k, in order to combine the signal fields into a common spatial mode with a relative phase ϕ_s, coupled to the optical fiber for detection.

After a 150 ns delay, two 200 ns long *read* pulses generated by the *read* AOD aligned in +1 Bragg order with frequencies f_j and f_k are sent through the two elements to convert the atomic excitations to the idler fields. The idler AOD, driven at at frequencies f_j and f_k, combines the idler frequency components into a single spatial mode, with a relative phase ϕ_i.

The rf phase shifters on the signal and idler AODs allow to vary ϕ_s and ϕ_i. The photoelectric coincidence counts of signal and idler fields as a function of these phases is shown in Fig. 5. We have measured violation of

Bell's inequality ($|S| \leq 2$), with $S_{exp} = 2.38 \pm 0.03$. Table 3.2 shows the interference fringe visibility V for different combinations of elements.

Table 3. Measured interference visibility with different combinations of quantum memory elements.

j	k	fringe visibility
5	8	$88 \pm 1\%$
7	8	$86 \pm 2\%$
7	10	$79 \pm 1\%$
5	10	$81 \pm 2\%$
1	12	$73 \pm 3\%$

4. Conclusion

We have observed a quantum memory with a lifetime in excess of six milliseconds and used it to implement a high-quality deterministic single photon source. We have also demonstrated matter-light entanglement with a quantum memory array in a single cold atomic sample.

This work was supported by the National Science Foundation, A. P. Sloan Foundation, Office of Naval Research, and the Army Research Office through the Georgia Tech Quantum Institute.

References

1. M. A. Nielsen and I. L. Chuang, *Quantum Computation and Quantum Information* (Cambridge University Press, 2000).
2. H.-J. Briegel, W. Dür, J. I. Cirac and P. Zoller, *Phys. Rev. Lett.* **81**, 5932 (1998).
3. L.-M. Duan, M. D. Lukin, J. I. Cirac and P. Zoller, *Nature* **414**, 413 (2001).
4. D. N. Matsukevich and A. Kuzmich, *Science* **306**, 663-666 (2004).
5. D. N. Matsukevich *et al.*, *Phys. Rev. Lett.* **96**, 030405 (2006)
6. T. Chanelière *et al.*, *Phys. Rev. Lett.* **96**, 093604 (2006).
7. O. A. Collins, S. D. Jenkins, A. Kuzmich and T. A. B. Kennedy, *Phys. Rev. Lett.* **98**, 060502 (2007).
8. D. N. Matsukevich *et al.*, *Phys. Rev. Lett.* **97**, 013601 (2006).
9. T. Chanelière *et al.*, *Nature* **438**, 833 (2005).
10. D. N. Matsukevich *et al.*, *Phys. Rev. Lett.* **95**, 040405 (2005).
11. D. N. Matsukevich *et al.*, *Phys. Rev. Lett.* **96** 033601 (2006).
12. T. Chanelière, D. N. Matsukevich, S. D. Jenkins, S.-Y. Lan, R. Zhao, T. A. B. Kennedy and A. Kuzmich, *Phys. Rev. Lett.* **98**, 113602 (2007).
13. Y. A. Chen *et al.*, *Nat. Phys.* **4** 103–107 (2007).

14. J. Simon, H. Tanji, S. Ghosh and V. Vuletic, *Nat. Phys.* **3** 765 (2007).
15. J. Laurat *et al.*, *Phys. Rev. Lett.* **99**, 180504 (2007).
16. M. Aspelmeyer *et al.*, *Science* **301**, 621 (2003).
17. S. Kuhr *et al.*, *Phys. Rev. A* **72**, 023406 (2005).
18. P. Grangier, G. Roger and A. Aspect, *Europhys. Lett.* **1**, 173 (1986).